Removal of the drug procaine from acidic aqueous solutions using a flow reactor with a boron-doped diamond anode

Nathalia M. P. Queiroz,[a] Ignasi Sirés,[b] Carmem L. P. S. Zanta,[c] Josealdo Tonholo,[c] Enric Brillas[b,*]

[a] *Technology Center, Federal University of Alagoas, CEP 57072-970, Maceió-Al, Brazil*

[b] *Laboratori d'Electroquímica dels Materials i del Medi Ambient, Departament de Química Física, Facultat de Química, Universitat de Barcelona, Martí i Franquès 1-11, 08028 Barcelona, Spain*

[c] *Institute of Chemistry and Biotechnology, Federal University of Alagoas, CEP 57072-970, Maceió-Al, Brazil*

Corresponding author: * brillas@ub.edu (E. Brillas)

Abstract

This article reports the electrochemical advanced oxidation treatment of 2.5 L of acidic aqueous solutions with 0.320 mM of the drug procaine hydrochloride in 0.050 M Na_2SO_4 using a pre-pilot flow plant. This was equipped with a cell, containing a boron-doped diamond (BDD) anode and an air-diffusion cathode for H_2O_2 generation, which was connected to an annular photoreactor with a 160 W UVA lamp for the study of photoelectro-Fenton (PEF) process. Poor degradation and mineralization was attained by electrochemical oxidation with electrogenerated H_2O_2 due to the limited attack of both, hydroxyl radical ($^{\bullet}OH$) formed at the BDD surface from water oxidation and H_2O_2 on organic matter. The electro-Fenton process became more effective thanks to the simultaneous oxidation with $^{\bullet}OH$ formed from Fenton's reaction in the presence of Fe^{2+}. The most powerful process was PEF because of the additional photolysis of photoactive intermediates by UVA radiation. This method allowed achieving 91% mineralization after 360 min of electrolysis at 33.3 mA cm^{-2}. The effect of current density and drug concentration on PEF performance was examined. The mineralization current efficiency and energy consumption were determined for each treatment. Two nitroderivatives were identified by gas chromatography-mass spectrometry. The quantification of generated carboxylic acids revealed that the final solution in PEF was composed of a mixture of acetic and formic acids.

Keywords: Electrochemical oxidation; Electro-Fenton; Photoelectro-Fenton; Procaine; Water treatment

1. Introduction

Procaine (2-(diethylamino)ethyl-4-aminobenzoate, see molecular structure in Table 1) is a local anesthetic drug widely used since its synthesis in 1905 that acts as a sodium channel blocker. It is commercially available as procaine hydrochloride ($C_{13}H_{20}N_2O_2 \cdot HCl$, M = 272.77 g mol^{-1}). It was first used to diminish the pain upon intramuscular injection of penicillin and later, in dentistry, although it also possesses therapeutic properties because of its mood- and perfusion-enhancing, anti-inflammatory, and sympatholytic effects. Procaine can be lethal at high doses (> 10 mg kg^{-1} for horses) since it can produce cardiac or respiratory arrests in human beings and animals, along with intoxication by the metabolites formed [1-3]. 4-Aminobenzoic acid, ethanolamine, monoethyl-aminoethanol, and diethylaminoethanol are the main metabolites found in animals such as rats, pigs, and horses [4,5]. Procaine has been detected at concentrations near 1 μg L^{-1} in industrial pharmaceutical wastewater [6,7] and effluents from wastewater treatment plants (WWTPs) [8]. The high stability of this drug under natural conditions along with its scarce removal in WWTPs explain its presence in the aquatic environment, although its potentially toxic effects on aquatic organisms have not been documented so far. The efficient removal of procaine and its products from industrial pharmaceutical wastewater by powerful transformation treatments seems necessary to avoid its discharge into natural water. Nonetheless, no specific technologies have been tested to destroy this drug. Worth noting, a single work has been reported on procaine hydrochloride degradation, using *N*-chlorobenzenesulfonamide in acid and alkaline media [9], but no previous studies have addressed the potential destruction of this compound by strong oxidants like hydroxyl radical ($^{\bullet}OH$). On the other hand, aqueous solutions with formulations (1:1) of procaine-penicillium G have been treated by chemical and photochemical advanced oxidation processes (AOPs) such as ozonation at pH 7 [10] and Fenton-like and photo-Fenton like at pH 3.0 [11]. The strong oxidant $^{\bullet}OH$ produced in situ by these methods yielded a partial mineralization (82% as

maximal) of such solutions, which contained 600 mg L^{-1} chemical oxygen demand (COD) and 450 mg L^{-1} total organic carbon (TOC). As an interesting finding, all treated solutions became biodegradable from acute toxicity tests with *Daphnia magna*, but neither products nor released inorganic ions were analyzed, and the oxidation of procaine in the complex formulation was not clarified either. This is an important issue that needs to be addressed in order to limit the duration of the oxidation method for subsequent combination with a less expensive biological post-treatment [12].

Over the last decade, powerful electrochemical AOPs (EAOPs) are being developed for the remediation of pharmaceuticals wastewater [12-16]. Among them, Fenton-based treatments with H_2O_2 electrogeneration seem the most promising EAOPs for industrial implementation [12-15]. In these processes, Fe^{2+} is added to the solution to react with H_2O_2 produced at the cathode of the electrochemical cell, eventually forming homogeneous $^{\bullet}OH$ via the well-known Fenton's reaction. The continuous production of H_2O_2 is ensured once O_2 gas is fed into the solution or through the cathode surface to be cathodically reduced to H_2O_2 via reaction (1) [12,14,15]. Carbonaceous cathodes show a high electrocatalytic activity for this reaction. Examples include carbon nanotubes [17,18], reticulated vitreous carbon [19], carbon and graphite felt [19-23] and carbon-polytetrafluoroethylene (PTFE) air-diffusion devices [22,24-27].

$$O_{2(g)} + 2H^+ + 2\,e^- \rightarrow H_2O_2 \qquad (1)$$

Other key factors that affect the effectiveness of EAOPs in undivided cells are the anode material and the electrolyte composition [28,29]. In the absence of chloride ions, boron-doped diamond (BDD) thin films are the best anodes [12-15]. The weak $^{\bullet}OH$-BDD interaction and the large overpotential for water discharge at BDD favor the generation of physisorbed hydroxyl radical (BDD($^{\bullet}OH$)) from reaction (2), which is more active than the radical adsorbed on

conventional Pt and dimensionally stable anodes (DSA®) [28-32]. In chlorinated media, the latter anodes become more effective to produce active chlorine, which reacts with organics in concomitance with heterogeneous $^{\bullet}OH$. However, the preferred anode also in this case is usually BDD since it possesses greater ability to remove the toxic and recalcitrant chloroderivatives formed. As a potential drawback, undesirable chlorate and perchlorate ions may be formed if the electrolysis conditions are not carefully controlled [33-36].

$$BDD + H_2O \rightarrow BDD(^{\bullet}OH) + H^+ + e^- \quad (2)$$

This work aims to assess whether the hydroxyl radicals generated by EAOPs, either alone or in concomitance with UVA light, are able to effectively degrade and mineralize acidic aqueous solutions of procaine at pH 3.0. Tests were carried out in a 2.5 L pre-pilot flow plant containing an undivided filter-press cell with a BDD anode and a carbon-PTFE cathode, which provided H_2O_2 to the solution from reaction (1). A typical non-chlorinated medium such as 0.050 M Na_2SO_4 was chosen to characterize the oxidation action of hydroxyl radicals produced, without significant interference of weaker oxidizing agents like persulfate ($S_2O_8^{2-}$) and sulfate radical ion ($SO_4^{\bullet-}$) coming from sulfate oxidation [12-15]. No other aqueous matrices (e.g., urban wastewater) were tested, in order to avoid the interference of active chlorine originated from the anodic oxidation of Cl^- ions [37]. Two Fenton-based EAOPs were compared, namely electro-Fenton (EF) and photoelectro-Fenton (PEF) under UVA (λ_{max} = 360 nm) irradiation. They were operated in the presence of 0.50 mM Fe^{2+}, the optimum content for Fenton's reaction using this kind of cell [38]. A drug concentration of 0.320 mM (i.e., 50 mg L^{-1} TOC), much higher than that found in the environment, was employed in order to determine the mineralization current efficiencies and energy consumptions related to the procaine removal, as well as to minimize the error in the analysis of the oxidation products formed and inorganic ions released. Comparative treatments in the absence of Fe^{2+} catalyst, i.e., electrochemical

oxidation with electrogenerated H_2O_2 (EO-H_2O_2), were also made in order to clarify the behavior of BDD($^{\bullet}$OH) and homogeneous $^{\bullet}$OH. For the most powerful process, the effect of applied current density (*j*) and drug concentration on its performance was assessed to understand the role of UVA radiation. Gas chromatography-mass spectrometry (GC-MS) was used to identify the aromatic products produced, whereas high-performance liquid chromatography (HPLC) was employed for the quantification of the final short-chain aliphatic carboxylic acids.

2. Materials and methods

2.1. Reagents

Procaine hydrochloride (99% purity) was provided by Sigma-Aldrich and used as received. The supporting electrolyte (Na_2SO_4) and Fenton's catalyst ($FeSO_4 \cdot 7H_2O$) were of analytical grade purchased from Fluka and Panreac. Analytical grade standard carboxylic acids were purchased from Merck and Panreac. The solutions treated in the 2.5 L pre-pilot flow plant were prepared with deionized water, whereas analytical solutions were prepared with Millipore Milli-Q ultrapure water (resistivity > 18.2 MΩ cm). Other reagents and chemicals were either of HPLC or analytical grade from Merck, Panreac and Prolabo.

2.2. Pre-pilot flow plant

The electrochemical assays were carried out in a 2.5 L pre-pilot flow plant constructed in our laboratory and containing the same basic elements as previously reported [39]. Briefly, the electrochemical cell was an undivided filter-press reactor with two electrodes of 20 cm^2 of exposed area, separated 1.2 cm. The cell was connected to a reservoir containing the solution through two heat-exchangers, which were fed with external water at constant temperature regulated with a Digiterm 3000542 thermostat from J.P. Selecta, a flowmeter and a peristaltic pump. The outlet of the cell was connected to an annular glass photoreactor of 640 mL, which

was either covered with an opaque cloth in EO-H_2O_2 and EF or equipped with a 27 E 160-W UVA lamp (320–400 nm, λ_{max} = 360 nm) from Omnilux to illuminate the solution in the PEF process. This lamp provided an irradiance of 134 W m^{-2}, as detected with a Kipp & Zonen CUV 5 radiometer. The anode was a BDD thin film on a Si wafer from NeoCoat (Le-Chaux-de-Fonds, Switzerland) and the cathode was a carbon-PTFE air-diffusion electrode from E-TEK (Somerset, NJ, USA), which was fed with air pumped at 8.6 kPa of overpressure to continuously produce H_2O_2 from reaction (1). An N5746A System DC power from Agilent Technologies was used to provide constant current to the cell, also measuring the potential difference between electrodes (E_{cell}). Before the trials, the two fresh electrodes were cleaned and activated in 0.050 M Na_2SO_4 at j = 100 mA cm^{-2} for 240 min. All the electrochemical assays were carried out in duplicate and the corresponding mean values of the parameters measured are reported in this work. The error bars with 95% confidence interval are included in figures.

2.3. Analytical methods

The solution pH was adjusted to 3.0 with analytical grade H_2SO_4 (Merck) and monitored during all the trials using a 2000 pH-meter from Crison. The H_2O_2 accumulated in the solution was measured by the standard metavanadate method using a 1800 UV/Vis spectrophotometer from Shimadzu set at λ = 450 nm [40].

For the degradation experiments, the samples were diluted (1:1) with acetonitrile to stop the oxidation and filtered with 0.45 μm PTFE filters from Whatman before HPLC analysis. This was made by injecting 10 μL aliquots into a 600 LC coupled to a 996 photodiode array detector (PDA) selected at λ = 290 (the maximum wavelength for procaine), both from Waters. The LC contained an ODS Hypersil 5 μm, 150 mm × 3 mm (i.d.), column from Thermo Electron Corporation at 25 ºC. A 60:40 (v/v) acetonitrile/water (10 mM KH_2PO_4, pH 3) mixture was circulated at 1 mL min^{-1} as mobile phase. Under these conditions, the procaine peak in the chromatograms appeared at a retention time t_r = 4.2 min, with L.O.D. = 0.085 mg L^{-1} and L.O.Q.

= 0.290 mg L^{-1}. Generated carboxylic acids were detected by injecting 20 μL samples into the same LC with an Aminex HPX 87H, 300 mm × 7.8 mm (i.d.), column from Bio-Rad at 35 ºC, and the PDA set at λ = 210 nm. A 4 mM H_2SO_4 solution at 0.6 mL min^{-1} was employed as mobile phase. Oxalic (t_r = 6.9 min), formic (t_r = 14.1 min) and acetic (t_r = 15.4 min) acids were quantified. NH_4^+, NO_3^-, and Cl^- contents in solution were measured following the procedures previously described [25,36].

TOC of solutions was measured on a TOC VCSN analyzer from Shimadzu upon injection of filtered 50 μL samples after immediate withdrawal from treated solutions. Reproducible values with ±1% accuracy were always obtained using the non-purgeable organic carbon (NPOC) method, with L.O.D. = 0.215 mg L^{-1} and L.O.Q. = 0.713 mg L^{-1}.

The stable organic components accumulated in 0.320 mM drug solutions with 0.050 M Na_2SO_4 at pH 3.0 upon EO-H_2O_2 treatment at j = 33.3 mA cm^{-2} were identified by GC-MS using a NIST05 library. Several samples of 100 mL were withdrawn at different electrolysis times and, for each one, the remaining organics were extracted with dichloromethane (3 × 25 mL) and further treated for volume reduction to about 2 mL. A 6890 N GC coupled to a 5975C inert XL MS, both from Agilent Technologies, was used for the GC-MS analysis. Organics were detected using a non-polar Sapiens-X5ms 0.25 μm, 30 m × 0.25 mm (i.d.), column from Teknokroma, as reported elsewhere [36].

3. Results and discussion

3.1. Comparative treatment of procaine solutions by EAOPs

Preliminary assays were performed to ensure the photostability of procaine in acidic aqueous medium and the ability of the electrolytic cell to generate H_2O_2 in the pre-pilot flow plant. A solution of 2.5 L of 0.320 mM procaine hydrochloride in 0.050 M Na_2SO_4 at pH 3.0 was recirculated through the plant equipped with a BDD/air-diffusion cell (20 cm^2 of exposed area

each) and connected to an annular glass photoreactor (irradiated volume of 640 mL) with a 160-W UVA lamp in its center. After 8 h at a liquid flow rate of 180 L h^{-1} and with intermittent 2-h exposure to UVA radiation, no change of absorbance in the UV spectrum of drug solution at λ_{max} = 290 nm was found, thus confirming its stability under the experimental conditions tested.

Another series of trials was made by electrolyzing 2.5 L of 0.050 M Na_2SO_4 at pH 3.0 in the above pilot plant at different *j* values without UVA irradiation, i.e., under EO-H_2O_2 conditions. Fig. 1 evidences a progressive increase in accumulated H_2O_2 at each *j* for 360 min, attaining final contents of 13.4, 25.7 and 31.1 mM at raising *j* values of 33.3, 66.7 and 100 mA cm^{-2}, respectively. Such enhancement can be related to the concomitant increase in rate of reaction (1). It is noticeable that each profile tended to a maximum value as a result of the gradual destruction of H_2O_2 in solution and, pre-eminently, at the anode surface where it was oxidized to O_2 via hydroperoxyl radical ($HO_2^{\bullet}$) production [12,14]. However, the amount of H_2O_2 accumulated was not proportional to the increase of current density, which is also due to the enhancement of H_2O reduction to H_2 gas at the cathode. This loss in current efficient was more significant as *j* was increased, and hence, current densities > 100 mA cm^{-2} were not useful in practice for H_2O_2 production. Despite this, the amount of H_2O_2 produced was high enough in all cases to generate a large quantity of homogeneous $^{\bullet}OH$ via Fenton's reaction during the EF and PEF treatments, which was also favored by the fast Fe^{2+} regeneration from Fe^{3+} reduction at the cathode [14-16].

Once studied the H_2O_2 production in the system, 0.320 mM drug solutions were electrolyzed under the above conditions by EO-H_2O_2, EF and PEF at *j* = 33.3 mA cm^{-2}. The two latter trials were carried out in the presence of 0.50 mM Fe^{2+} as catalyst. No significant pH change, close to 3.0, was found after 360 min of such electrolyses. Fig. 2a depicts a very slow decay of drug concentration upon EO-H_2O_2 treatment, attaining only 45% removal at 60 min. This informs about the very small reaction rate of procaine with physisorbed BDD($^{\bullet}OH$)

originated from reaction (2). At the same treatment time, total drug removal was reached by EF due to its much faster reaction with homogeneous $^{\bullet}OH$ formed from Fenton's reaction (3) with Fe^{3+} production [12,41,42].

$$Fe^{2+} + H_2O_2 \rightarrow Fe^{3+} + {}^{\bullet}OH + OH^{-} \quad (3)$$

Fig. 2a also highlights the slightly quicker abatement of the drug by PEF, which disappeared in 45 min. In this process, a greater amount of homogeneous $^{\bullet}OH$ is generated to more rapidly destroy the photostable procaine molecule. This can be accounted for by the occurrence of reaction (4), in which $[Fe(OH)]^{2+}$, the most stable Fe^{3+} species at pH 3.0, originated from reaction (3), is photoreduced by UVA light to $^{\bullet}OH$ and Fe^{2+} with the consequent acceleration of the catalytic Fe^{3+}/Fe^{2+} cycle [14,27,37].

$$[Fe(OH)]^{2+} + h\nu \rightarrow Fe^{2+} + {}^{\bullet}OH \quad (4)$$

The procaine concentration profiles show an exponential trend in both Fenton-based EAOPs (Fig. 2a), which can then be interpreted considering a pseudo-first-order reaction kinetics, as presented in Fig. 2b. From the linear regression, the apparent rate constants (k) for procaine removal were determined. Table S1 shows k-values of $(7.55\pm0.36)\times10^{-2}$ min^{-1} in EF and $(7.99\pm0.42)\times10^{-2}$ min^{-1} in PEF, with good R^2-values. This suggests the formation of a small and steady concentration of $^{\bullet}OH$ from reactions (3) and/or (4) to destroy the target molecule. A different behavior can be observed in Fig. 2b in the case of EO-H_2O_2, since a non-linear ln (c_0 /c) vs. time plot was found. This is due to a progressive decay of the procaine removal rate as the treatment was prolonged, probably because the oxidant BDD($^{\bullet}OH$) attacked more rapidly its products, lowering its availability to oxidize the drug.

The percentage of mineralization in the above assays was monitored by determining the TOC abatement for 360 min, a time much longer than that required for degradation because of

the great recalcitrance of the oxidation products generated. Fig. 3a depicts a gradual TOC disappearance in all cases. Table S1 also depicts a decreasing oxidation ability of the EAOPs in the order: PEF >> EF > EO-H_2O_2. The less powerful treatment was EO-H_2O_2 and hence, all organics were quite refractory even to BDD($^{\bullet}$OH) since only 26% TOC removal was achieved after 360 min of electrolysis. In the presence of Fe^{2+}, i.e., under EF conditions, the additional attack of homogeneous $^{\bullet}$OH caused a more rapid mineralization of organics, attaining 54% TOC decay. The PEF treatment had the greatest mineralization power, giving rise to 91% TOC abatement at 360 min (see Table S1). This corroborates the huge impact of UVA radiation on the process performance, thanks to photolysis of some by-products, whereas these species are slowly attacked by BDD($^{\bullet}$OH) and $^{\bullet}$OH, as revealed by EO-H_2O_2 and EF profiles. Fig. 3a also shows that in PEF, TOC decreased quickly until 240 min, whereupon its decay was strongly decelerated, suggesting the formation of highly persistent products that are very slowly removed [14,27-29].

For each mineralization process, the conversion of the two *N* atoms of procaine in 0.320 mM solutions into inorganic ions was assessed. Analysis of treated solutions only allowed detecting the release of NH_4^+ ion. Neither NO_2^- nor NO_3^- ions were found. The time course of NH_4^+ concentration obtained in all the above treatments is shown in Fig. 3b. This ion was quickly released at the beginning of all treatments, progressively decreasing its accumulation rate at longer time. The final amount of NH_4^+ was increased at a greater oxidation ability of the EAOPs because larger quantities of *N*-derivatives were mineralized. Final values of 0.261 mM (40.8% of initial N) in EO-H_2O_2, 0.288 mM (45.0% of initial N) in EF, and 0.332 mM (51.9% of initial N) in PEF were obtained. Taking into account that 91% TOC was removed by the latter process (Fig. 3a), the loss of volatile *N*-products, e.g., N_2 and N_xO_y, can be inferred, as previously proposed for other *N*-compounds [24,27,36,37].

The evolution of Cl^- ion during the EAOPs tested was determined as well. Fig. 3c reveals that, in all cases, the initial Cl^- concentration (0.320 mM) was slowly removed by less than 9%, as expected from the very low content of active chlorine formed from the anodic oxidation of this ion [34-36]. That confirms that the main oxidizing agents in the EAOPs are heterogeneous BDD($^{\bullet}OH$) formed from reaction (2) and/or homogeneous $^{\bullet}OH$ generated from Fenton's reaction (3) and reaction (4), with additional photolytic reactions induced by UVA light in PEF.

3.2 Mineralization current efficiency and energy consumption

From the findings reported in subsection 3.1, the following reaction can be written for the total mineralization of protonated procaine molecule, the species present in solution, considering the formation of NH_4^+ ion:

$$C_{13}H_{21}N_2O_2^+ + 24H_2O \rightarrow 13CO_2 + 2NH_4^+ + 61H^+ + 62e^- \quad (5)$$

Reaction (5) shows that the number (n) of transferred electrons for procaine mineralization is 62. Based on this, the percentage of mineralization current efficiency (MCE) was estimated for all trials as follows [37]:

$$\text{MCE} = \frac{n\,F\,V\,\Delta\text{TOC}}{4.32\times10^7\,m\,I\,t}\,100 \quad (6)$$

where ΔTOC is the TOC abatement (in mg L^{-1}) at applied current I (in A) for a given time t (in h). The constant values in Eq. (6) are the Faraday constant F, the solution volume V (2.5 L), a conversion factor (= 3600 s h^{-1} x 12,000 mg C mol^{-1}) and the number of carbon atoms (m = 13).

Fig. 4a shows the MCE values calculated from Eq. (6) for the tests of Fig. 3a. The EO-H_2O_2 process showed a steady MEC value near 8-9% from 180 min of electrolysis (see Table S1), suggesting that all organic molecules are mineralized at similar rate under such conditions. This behavior is not observed in EF and PEF, which present maximum MCE values of 28.0% and 76.8% between 60 and 120 min, respectively, i.e., when the maximum mineralization rate

was achieved. This means that the destruction of readily oxidizable compounds was accelerated until the maximum MCE value was attained. At longer time, the MCE decayed gradually, although more dramatically in PEF down to 29.2%, still greater than 17.5% determined in EF at 360 min (see Table S1) This loss of current efficiency can be related to two factors [14,16]: (i) the abatement of the dissolved organic load, and (ii) the generation of final products, being so highly recalcitrant that they can only be very slowly removed by the different oxidizing agents and UVA photons.

The energy consumption per unit TOC mass (EC_{TOC}, in kWh (g TOC)$^{-1}$) for each experiment was calculated from Eq. (7) [37]:

$$EC_{TOC} = \frac{E_{cell}\, I\, t}{V\, \Delta TOC} \qquad (7)$$

where E_{cell} denotes the potential difference between the electrodes of the cell (in V) and the rest of parameters have been defined above. Note that this equation has also been employed for calculation in PEF treatment, but without considering the energy related to the 160-W lamp. For the real application at a larger scale, the solar PEF (SPEF) process using free sunlight could be alternatively utilized. Under such conditions, no additional energy consumption from light irradiation should be considered and Eq. (7) would give an idea of the energy requirements for the treatment [14,27,37].

The EC_{TOC} values present an opposite tendency as compared to the MCE ones, thus reaching minimal values as the MCE became maximal. Fig. 4b shows the high energy consumption of about 1 kWh (g TOC)$^{-1}$ determined for EO-H_2O_2 treatment at times ≥ 120 min, which is due to its very low mineralization ability (see also Table S1). At shorter time, much higher EC_{TOC} values were obtained, e.g., 5.71 kWh (g TOC)$^{-1}$ at 40 min. As expected, the EC_{TOC} in EF and PEF was drastically smaller, with minimal values of 0.292 kWh (g TOC)$^{-1}$ at 120 min and 0.106 kWh (g TOC)$^{-1}$ at 90 min, respectively, which gradually rose up to 0.468 and 0.279 kWh (g TOC)$^{-1}$ at the end of treatments (see Table S1). According to these results, the

most powerful EAOP, i.e., PEF process, was not only the most efficient but also the less expensive treatment, disregarding the energy associated with the UVA lamp. If the electric energy from the lamp was taken into account, the energy consumption of 8.81 kWh (g TOC)$^{-1}$ would be excessively high for industrial application. Hence, its alternative use with sunlight can be envisaged as the best method for the decontamination of wastewater containing procaine.

3.3 Effect of current density and drug concentration on PEF performance

Once established that PEF was the best method for procaine mineralization, the influence of key variables on its performance was assessed in order to know the role of generated hydroxyl radicals and UVA radiation during the process. The first variable to be tested was *j*, since it limits the concentration of physisorbed BDD($^{\bullet}$OH) and homogeneous $^{\bullet}$OH produced in the electrolytic system. Trials were then carried out between 33.3 and 100 mA cm^{-2} and the evolution of normalized TOC decay with time is depicted in Fig. 5a. Surprisingly, very similar profiles can be observed for TOC abatement as *j* was increased, reaching final removals between 91% and 94% from 33.3 to 100 mA cm^{-2}, respectively (see Table S1). This means that the mineralization process is mainly controlled by the action of UVA radiation over the photoactive intermediates. Therefore, the excess of BDD($^{\bullet}$OH) and $^{\bullet}$OH generated upon enhancement of reactions (1)-(4), as *j* was increased, was mainly wasted in their non-oxidizing parasitic reactions. These include, for example, the anodic oxidation of BDD($^{\bullet}$OH) to BDD and O_2 and the attack of homogeneous $^{\bullet}$OH over H_2O_2 and Fe^{2+} [14,15,24]. The results suggest that the enhancement of such parasitic reactions occurs because a large proportion of products are photoactive and then, more rapidly photodecomposed by UVA light than oxidized by hydroxyl radicals. Moreover, it seems that at the end of treatment (times longer than 240 min) the remaining products are so highly recalcitrant that can only be very slowly removed by the different oxidizing agents and UVA photons.

The profiles of MCE and EC_{TOC} vs. electrolysis time for the above tests are presented in Fig. 5b and 5c, respectively. As can be seen, the rise of *j* did not favor the PEF treatment, because MCE gradually decreased and EC_{TOC} underwent a high growth because of the increase of E_{cell}. Regarding MCE, Fig. 5b highlights that maximum values of 76.8%, 42.7% and 28.6% at about 90 min were found at 33.3, 66.7 and 100 mA cm^{-2}, respectively, whereas they dropped to final values from 29.2% to 10.2% (see Table S1). The fact that the maximum of MCE was reached at a similar time with increasing *j* can be explained by the quicker mineralization of the easily oxidizable products in the presence of the greater amounts of BDD($^{\bullet}$OH) and $^{\bullet}$OH produced. However, the generation of recalcitrant photoactive products caused that the overall process was subsequently limited by their photodecomposition, with little influence of hydroxyl radicals and hence, of *j*. This can also explain the minimum values of 0.106, 0.305 and 0.650 kWh (g TOC)$^{-1}$ determined at the same time. Fig. 5c evidences that at longer time, the energy consumption always increased, reaching a value as high as 1.867 kWh (g TOC)$^{-1}$ at j = 100 mA cm^{-2}, in contrast to 0.279 kWh (g TOC)$^{-1}$ determined at j = 33.3 mA cm^{-2} (see Table S1).

All the above findings indicate that the lowest *j* of 33.3 mA cm^{-2} was preferable under the present experimental conditions because it allowed a high TOC removal (91%) with much greater MCE and lower EC_{TOC} than higher *j* values.

Another critical variable is the initial drug concentration, since it allows evaluating the ability of PEF to mineralize highly concentrated organic products from the parent molecule. This was studied by electrolyzing from 0.064 to 0.320 mM procaine hydrochloride at the best j = 33.3 mA cm^{-2}. Fig. 6a shows a similar TOC removal at all organic loads, slightly increasing as the drug content was decreased but always attaining final reductions of 90-91% (see Table S1). This means that a growing quantity of TOC was destroyed with increasing drug content, being about 9.1 mg L^{-1} for solutions with 0.064 mM, 22.6 mg L^{-1} at 0.160 mM and 45.0 mg L^{-1} at 0.320 mM. Since the same contents of BDD($^{\bullet}$OH) and $^{\bullet}$OH are expected to be formed

because the same *j* was applied in all cases, one can infer that their parasitic reactions are gradually inhibited and larger quantities of both reactive radicals are actually available to react with organic molecules. This behavior is confirmed from the enhancement of the MCE values, as shown in Fig. 6b. Maximum values of 24.9% after 40 min starting with 0.064 mM, 43.0% after 60 min at 0.160 mM and 76.8% after 70 min at 0.320 mM were obtained, decreasing to 5.9%, 14.8%, and 29.2% at 360 min, respectively (see Table S1). The opposite tendency was followed by EC_{TOC}, as can be seen in Fig. 6c. The most expensive treatment was then obtained when treating 0.064 mM, since the EC_{TOC} value rose from about 0.35 kWh (g TOC)$^{-1}$ within the first hour of treatment to 1.372 kWh (g TOC)$^{-1}$ at 360 min. These energy consumptions decreased drastically at higher drug concentrations because of the greater efficiency of the PEF treatment, attaining 0.551 and 0.279 kWh (g TOC)$^{-1}$ after 360 min at 0.160 and 0.320 mM, respectively (see Table S1). Although it is clear that the performance of the treatment was improved at a higher organic content, it is noticeable the great ability of the system to effectively destroy low initial procaine concentrations, making it suitable for all kinds of initial conditions.

3.4 Detection of oxidation products

The primary stable oxidation products originated from the attack of hydroxyl radicals on the drug were identified in 0.320 mM procaine hydrochloride solutions electrolyzed by the less powerful EAOP, namely EO-H_2O_2, at j = 33.3 mA cm^{-2}. Table 1 collects the characteristics of the three organic compounds detected, including the parent molecule of procaine (**1**) that was very slowly removed by this method. The nitration of the –NH_2 group leads to compound **2**, which is subsequently oxidized to compound **3** with loss of the diethylamino group. The generation of these products could suggest the release of NO_3^- ion from the cleavage of the C(4)-N bond of the aromatic moiety. However, this ion was not detected in the treated solutions, as expected if its main release occurs via NH_4^+ and volatile N_xO_y species.

Another interesting aspect to be considered to clarify the fate of contaminants treated by EAOPs is the identification and quantification of the final products. It is expected that benzenic products are transformed into smaller aliphatic molecules, including short-chain carboxylic acids [12,14,15]. This possibility was explored by analyzing the electrolyzed solutions under the same conditions described in Fig. 3a by ion-exclusion HPLC. In the case of EO-H_2O_2, only small contents of oxalic acid (< 0.08 mM) were found between 150 and 360 min of electrolysis, which is not surprising taking into account the limited mineralization ability of this method. A very different behavior was observed in EF and PEF treatments, in which three carboxylic acids, namely acetic, formic and oxalic, were detected. In these EAOPs, a large proportion of iron is in the form of Fe^{3+} ion when an air-diffusion cathode is used and hence, most of the above acids are complexed with Fe(III) [14]. These species are not attacked by homogeneous $^{\bullet}OH$, are slowly mineralized by physisorbed BDD($^{\bullet}OH$), and some of them can be photodecarboxylated. Note that acetic acid is converted into oxalic and formic acids, which are final products that are directly transformed into CO_2 [14,27,39].

Fig. 7a and 7b present the profiles of the concentration of each carboxylic acid found in EF and PEF treatments, respectively. In the former treatment, a large and continuous accumulation of oxalic acid up to 17.8 mM can be observed. A smaller accumulation occurred for formic acid, reaching 9.5 mM as maximum concentration and finally dropping to 5.02 mM, whereas acetic acid disappeared from the medium after reaching a maximal of 4.8 mM at 240 min. A simple mass balance of the EF treatment revealed that all carboxylic acids contributed with 6.1 mg L^{-1} TOC to the final solution, only accounting for 26.5% of the remaining 23.0 mg L^{-1} of TOC (Fig. 3a). This means that, after the EF process, the solution still contained 16.9 mg L^{-1} of TOC related to other undetected and persistent products. Regarding the PEF treatment, Fig. 7b highlights that oxalic acid was not present in solution because of the rapid photolysis of Fe(III)-oxalate complexes. In contrast, high contents of acetic and formic acids were accumulated,

indicating that a large proportion of recalcitrant products that were not destroyed in EF could be photolyzed, thus largely enhancing the mineralization process in PEF. This can also be inferred from the mass balance of the final acetic and formic acids, with concentrations of 7.5 and 9.9 mM. This corresponded to 5.6 mg L^{-1} TOC, a value that agrees with the 100% of the TOC found for the final treated solution (Fig. 3a). In fact, this was already verified at 240 min, when the solution was already hardly mineralized. At that time, the sum of all acids yielded 7.0 mg L^{-1} TOC, very close to 7.5 mg L^{-1} of the TOC experimentally determined. This informs about the pre-eminent conversion of procaine hydrochloride into a mixture of acetic and formic acids in PEF. Therefore, for practical implementation, the duration of PEF could be shortened to be subsequently combined with a biological post-treatment. This would become a more cost-effective solution for industrial application. It should be noted that the complete conversion of an aromatic pollutant into carboxylic acids has been rarely reported in the literature. To our knowledge, this has been described for the SPEF treatment of the herbicide mecoprop at pH 3.0, yielding a final solution composed of acetic acid [39], which was hardly oxidized as also occurs here for the PEF treatment of procaine.

4. Conclusions

Hydroxyl radicals generated by EAOPs, pre-eminently those combined with UVA radiation, were very effective to treat acidic water contaminated with procaine. The PEF process had much greater oxidation ability than EF to decontaminate 2.5 L of 0.320 mM procaine in 0.050 M Na_2SO_4 with 0.50 mM Fe^{2+} at pH 3.0. At j = 33.3 mA cm^{-2}, 91% TOC removal was attained after 360 min of PEF with 29.2% MCE and 0.279 kWh (g TOC)$^{-1}$ of energy consumption. In contrast, only 54% TOC was abated using EF, meaning that a large proportion of recalcitrant species to BDD($^{\bullet}$OH) and $^{\bullet}$OH are photoactive and can be photodecomposed by UVA light in PEF. Procaine concentration dropped at similar rate in the two Fenton-based

methods, following a pseudo-first-order kinetics, owing to the action of $^{\bullet}OH$ as main oxidant. In EO-H_2O_2, much slower procaine and TOC decays were obtained, as expected if the drug and its products are hardly attacked by BDD($^{\bullet}OH$). NH_4^+ was the only dissolved nitrogenated ion detected, which was accompanied by two N-containing derivatives identified by GC-MS. Ion-exclusion HPLC analysis of treated solutions revealed that the final solution upon PEF treatment was composed of a mixture of only Fe(III)-acetate and Fe(III)-formate complexes, because of the total photodecarboxylation of Fe(III)-oxalate complexes.

Acknowledgements

The authors thank the economic support from project CTQ2016-78616-R (AEI/FEDER, EU). N. M. P. Queiroz also acknowledges funding from the Coordenação de Aperfeiçoamento de Pessoal de Nível Superior – Brasil (CAPES) – Finance Code 001, to do this work.

References

[1] I.L. Nielsen, K.A. Jacobs, P.J. Huntington, C.B. Chapman, K.C. Lloyd, Adverse reaction to procaine penicillin G in horses, Aust. Vet. J. 65 (1988) 181-185.

[2] Z.N. Ding, Y. Yoshita, K. Hirota, K. Yamamoto, T. Kobayashi, S. Murakami, Brainstem auditory evoked potentials during procaine toxicity in dogs, Can. J. Anesth. 39 (1992) 600-603.

[3] L. Olsen, C. Ingvast-Larsson, H. Brostroem, P. Larsson, H. Tjaelve, Clinical signs and etiology of adverse reactions to procaine benzylpenicillin and sodium/potassium benzylpenicillin in horses, J. Vet. Pharmacol. Ther. 30 (2007) 201-207.

[4] K. Kaemmerer, M. Kietzmann, Intermediary metabolic effects of procaine and its metabolites after oral administration, Z. Alternsforsch 44 (1989) 189-199.

[5] J.G. Zhang, W.E. Lindup, Effects of procaine and two of its metabolites on cisplatin-induced kidney injury in vitro: mitochondrial aspects, Toxicol. in Vitro 8 (1994) 477-481.

[6] S. Babic, D. Mutavdzic Pavlovic, D. Asperger, M. Perisa, M. Zrncic, A.J.M. Horvat, M. Kastelan-Macan, Determination of multi-class pharmaceuticals in wastewater by liquid chromatography–tandem mass spectrometry (LC–MS–MS), Anal. Bioanal. Chem. 398 (2010) 1185-1194.

[7] D. Asperger, V. Tisler, M. Zrncic, D. Mutavdzic Pavlovic, S. Babic, A.J.M. Horvat, M. Kastelan-Macan, HPLC–DAD–FLD determination of veterinary pharmaceuticals in pharmaceutical industry wastewater with precolumn derivatization using fluorescamine, Chromatographia 77 (2014) 1059-1066.

[8] R. Bade, J.M. White, C. Gerber, Qualitative and quantitative temporal analysis of licit and illicit drugs in wastewater in Australia using liquid chromatography coupled to mass spectrometry, Anal. Bioanal. Chem. 410 (2018) 529-542.

[9] Puttaswamy, J.P. Shubha, Kinetics of oxidation of procaine hydrochloride by sodium N-chlorobenzenesulfonamide in acid and alkaline media: A mechanistic approach, Indian J. Chem. 45A (2006) 2412-2417.

[10] I. Arslan-Alaton, A.E. Caglayan, Ozonation of Procaine Penicillin G formulation effluent Part I: Process optimization and kinetics, Chemosphere 59 (2005) 31-39.

[11] I. Arslan-Alaton, F. Gurses, Photo-Fenton-like and photo-fenton-like oxidation of Procaine Penicillin G formulation effluent, J. Photochem. Photobiol. A: Chem. 165 (2004) 165-175.

[12] O. Ganzenko, D. Huguenot, E.D. van Hullebusch, G. Esposito, M.A. Oturan, Electrochemical advanced oxidation and biological processes for wastewater treatment: a review of the combined approaches, Environ. Sci. Pollut. Res. Int. 21 (2014) 8493-8524.

[13] B. Ramesh Babu, P. Venkatesan, R. Kanimozhi, C. Ahmed Basha, Removal of pharmaceuticals from wastewater by electrochemical oxidation using cylindrical flow reactor and optimization of treatment conditions, J. Environ. Sci. Health A 44 (2009) 985-994.

[14] I. Sirés, E. Brillas, Remediation of water pollution caused by pharmaceutical residues based on electrochemical separation and degradation technologies: a review, Environ. Int. 40 (2012) 212-229.

[15] L. Feng, E.D.van Hullebusch, M.A. Rodrigo, G. Esposito, M.A. Oturan, Removal of residual anti-inflammatory and analgesic pharmaceuticals from aqueous systems by electrochemical advanced oxidation processes. A review, Chem. Eng. J. 228 (2013) 944-964.

[16] E. Brillas, I. Sirés, Electrochemical removal of pharmaceuticals from water streams: Reactivity elucidation by mass spectrometry, TrAC Trends Anal. Chem. 70 (2015) 112-121.

[17] A. Khataee, A. Khataee, M. Fathinia, B. Vahid, S.W. Joo, Kinetic modeling of photoassisted-electrochemical process for degradation of an azo dye using boron-doped diamond anode and cathode with carbon nanotubes, J. Ind. Eng. Chem. 19 (2013) 1890-1894.

[18] A. Khataee, A. Akbarpour, B. Vahid, Photoassisted electrochemical degradation of an azo dye using Ti/RuO_2 anode and carbon nanotubes containing gas-diffusion cathode, J. Taiwan Inst. Chem. Eng. 45 (2014) 930-936.

[19] G. Coria, T. Pérez, I. Sirés, J.L. Nava, Mass transport studies during dissolved oxygen reduction to hydrogen peroxide in a filter-press electrolyzer using graphite felt, reticulated vitreous carbon and boron-doped diamond as cathodes, J. Electroanal. Chem. 757 (2015) 225-229.

[20] M. Panizza, M.A. Oturan, Degradation of Alizarin Red by electro-Fenton process using a graphite-felt cathode, Electrochim. Acta 56 (2011) 7084-7087.

[21] M.S. Yahya, N. Oturan, K. El Kacemi, M. El Karbane, C.T. Aravindakumar, M.A. Oturan, Oxidative degradation study on antimicrobial agent ciprofloxacin by electro-Fenton process: kinetics and oxidation products, Chemosphere 117 (2014) 447-454.

[22] A. El-Ghenymy, R.M. Rodríguez, E. Brillas, N. Oturan, M.A. Oturan, Electro-Fenton degradation of the antibiotic sulfanilamide with Pt/carbon-felt and BDD/carbon-felt cells. Kinetics, reaction intermediates, and toxicity assessment, Environ. Sci. Pollut. Res. 21 (2014) 8368-8378.

[23] O. Ganzenko, N. Oturan, I. Sirés, D. Huguenot, E.D. van Hullebusch, G. Esposito, M.A. Oturan, Fast and complete removal of the 5-fluorouracil drug from water by electro-Fenton oxidation, Environ. Chem. Lett. 16 (2018) 281-286.

[24] A. Thiam, I. Sirés, F. Centellas, P.L. Cabot, E. Brillas, Decolorization and mineralization of Allura Red AC azo dye by solar photoelectro-Fenton: Identification of intermediates, Chemosphere 136 (2015) 1-8.

[25] A. Thiam, I. Sirés, J.A. Garrido, R.M. Rodríguez, E. Brillas, Effect of anions on electrochemical degradation of azo dye Carmoisine (Acid Red 14) using a BDD anode and air-diffusion cathode, Sep. Purif. Technol. 140 (2015) 43-52.

[26] S. Lanzalaco, I. Sirés, M.A. Sabatino, C. Dispenza, O. Scialdone, A. Galia, Synthesis of polymer nanogels by electro-Fenton process: investigation of the effect of main operation parameters, Electrochim. Acta 246 (2017) 812-822.

[27] J.R. Steter, E. Brillas, I. Sirés, Solar photoelectro-Fenton treatment of a mixture of parabens spiked into secondary treated wastewater effluent at low input current, Appl. Catal. B: Environ. 224 (2018) 410-418.

[28] G. Coria, I. Sirés, E. Brillas, J.L. Nava, Influence of the anode material on the degradation of naproxen by Fenton-based electrochemical processes, Chem. Eng. J. 304 (2016) 817-825.

[29] J. R. Steter, E. Brillas, I. Sirés, On the selection of the anode material for the electrochemical removal of methylparaben from different aqueous media, Electrochim. Acta 222 (2016) 1464-1474.

[30] B. Boye, P.A. Michaud, B. Marselli, M.M. Dieng, E. Brillas, C. Comninellis, Anodic oxidation of 4-chlorophenoxyacetic acid on synthetic boron-doped diamond electrodes, New Diamond Frontier Carbon Technol. 12 (2002) 63-72

[31] M. Panizza, G. Cerisola, Direct and mediated anodic oxidation of organic pollutants, Chem. Rev. 109 (2009) 6541-6569.

[32] S. Lanzalaco, I. Sirés, A. Galia, M.A. Sabatino, C. Dispenza, O. Scialdone, Facile crosslinking of poly(vinylpyrrolidone) by electro-oxidation with IrO_2-based anode under potentiostatic conditions, J. Appl. Electrochem. 48 (2018) 1343-1352.

[33] M.E.H. Bergmann, J. Rollin, T. Iourtchouk, The occurrence of perchlorate during drinking water electrolysis using BDD anodes, Electrochim. Acta 54 (2009) 2102−2107.

[34] S. Randazzo, O. Scialdone, E. Brillas, I. Sirés, Comparative electrochemical treatments of two chlorinated aliphatic hydrocarbons. Time course of the main reaction by-products, J. Hazard. Mater. 192 (2011) 1555-1564.

[35] H. Zöllig, A. Remmele, C. Fritzsche, E. Morgenroth, K.M. Udert, Formation of chlorination byproducts and their emission pathways in chlorine mediated electro-oxidation of urine on active and nonactive type anodes, Environ. Sci. Technol. 49 (2015) 11062-11069.

[36] C. Ridruejo, F. Centellas, P.L. Cabot, I. Sirés, E. Brillas, Electrochemical Fenton-based treatment of tetracaine in synthetic and urban wastewater using active and non-active anodes, Water Res. 128 (2018) 71-81.

[37] E.J. Ruiz, A. Hernández-Ramírez, J.M. Peralta-Hernández, C. Arias, E. Brillas, Application of solar photoelectro-Fenton technology to azo dyes mineralization: Effect of current density, Fe^{2+} and dye concentration, Chem. Eng. J. 171 (2011) 385-392.

[38] Z. Ye, E. Brillas, F. Centellas, P.L. Cabot, I. Sirés, Electrochemical treatment of butylated hydroxyanisole: Electrocoagulation versus advanced oxidation, Separ. Purif. Technol. 208 (2019) 19-26.

[39] C. Flox, J.A. Garrido, R.M. Rodríguez, P.L. Cabot, F. Centellas, C. Arias, E. Brillas, Mineralization of herbicide mecoprop by photoelectro-Fenton with UVA and solar light, Catal. Today 129 (2007) 29-36.

[40] R.F. Pupo Nogueira, M.C. Oliveira, W.C. Paterlini, Simple and fast spectrophotometric determination of H_2O_2 in photo-Fenton reactions using metavanadate, Talanta 66 (2005) 86-91.

[41] S. Vasudevan, M.A. Oturan, Electrochemistry: as cause and cure in water pollution-an overview, Environ. Chem. Lett. 12 (2014) 97-108.

[42] A. Galia, S. Lanzalaco, M.A. Sabatino, C. Dispenza, O. Scialdone, I. Sirés, Crosslinking of poly(vinylpyrrolidone) activated by electrogenerated hydroxyl radicals: A first step towards a simple and cheap synthetic route of nanogel vectors, Electrochem. Commun. 62 (2016) 64-68.

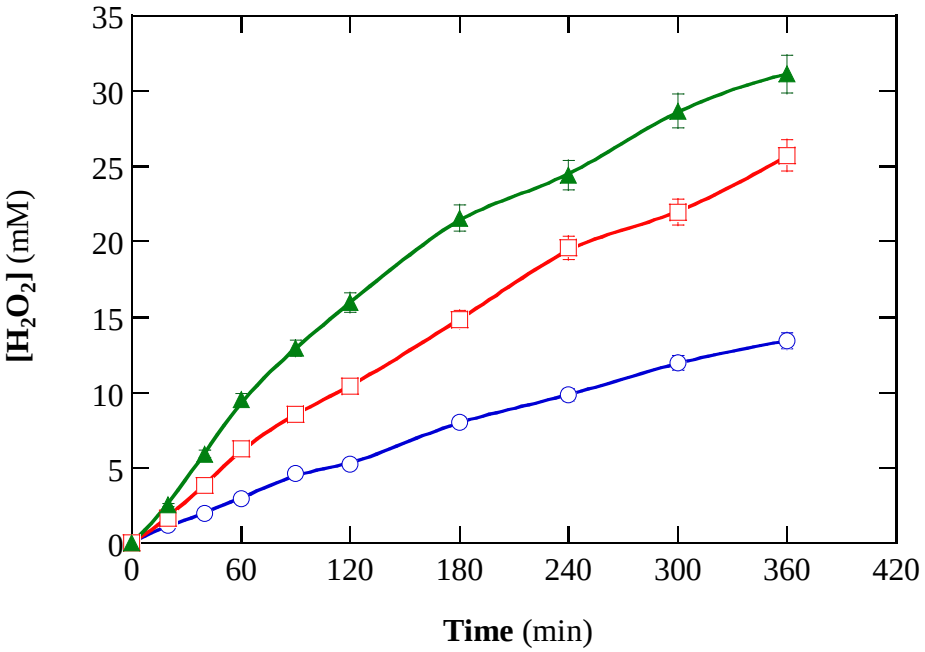

Fig. 1. Concentration of accumulated H_2O_2 vs. electrolysis time in 2.5 L of 0.050 M Na_2SO_4 at pH 3.0 and 35 ºC using a pre-pilot flow plant with an electrochemical reactor containing a BDD anode and an air-diffusion cathode, both of 20 cm^2, at liquid flow rate of 180 L h^{-1}. Current density: (○) 33.3 mA cm^{-2}, (□) 66.7 mA cm^{-2} and (▲) 100 mA cm^{-2}.

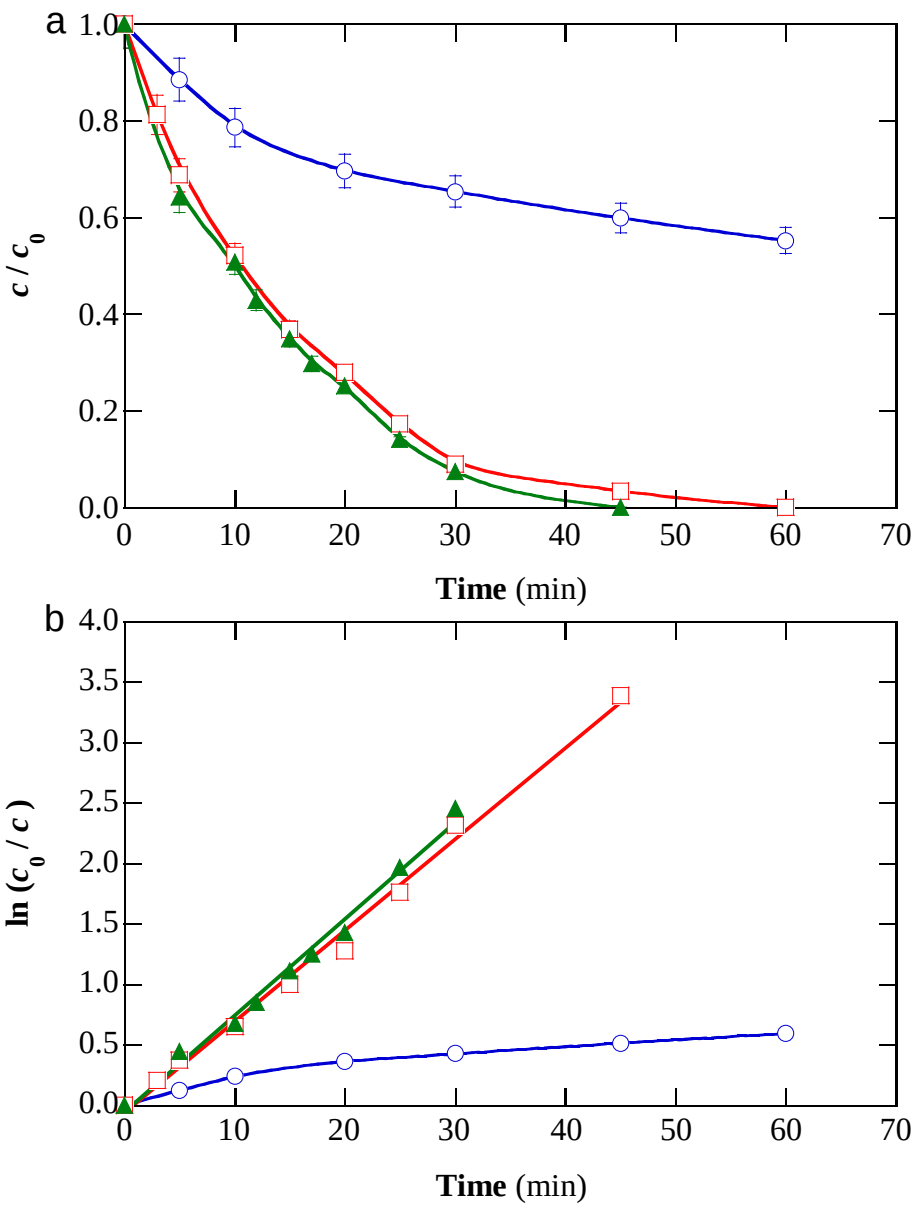

Fig. 2. (a) Normalized drug concentration decay vs. electrolysis time and (b) pseudo-first-order kinetic analysis for the degradation of 2.5 L of a 0.320 mM procaine hydrochloride solution with 0.050 M Na_2SO_4 at pH 3.0 and 35 ºC using a pre-pilot flow plant with a BDD/air-diffusion cell (20 cm^2 electrode area) at current density (*j*) of 33.3 mA cm^{-2} and liquid flow rate of 180 L h^{-1}. Method: (○) Electrochemical oxidation with electrogenerated H_2O_2 (EO-H_2O_2), (□) electro-Fenton (EF) and (▲) photoelectro-Fenton (PEF). The two latter trials were made with 0.50 mM Fe^{2+}. The PEF treatment was performed under irradiation with a 160-W UVA lamp.

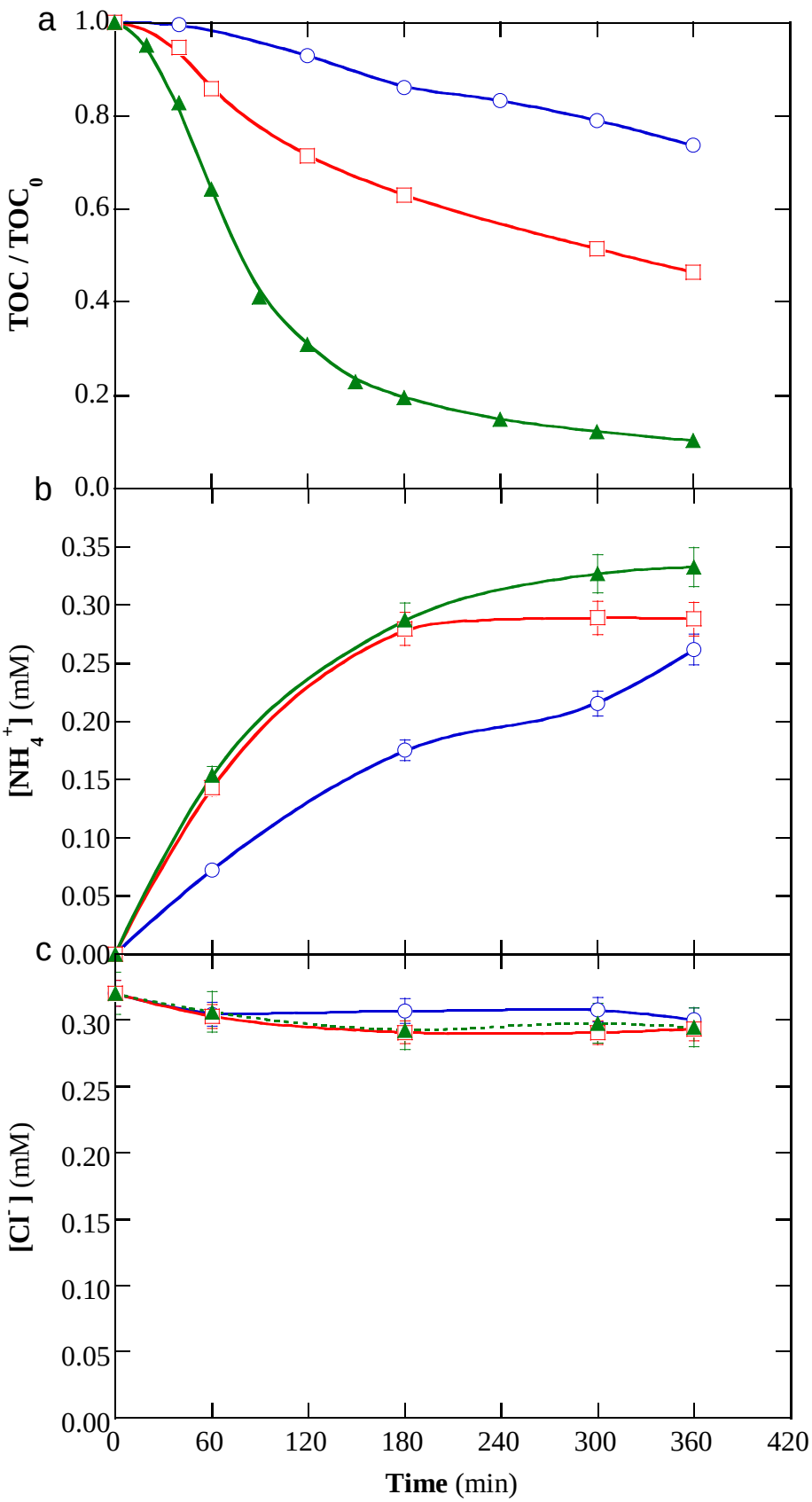

Fig. 3. (a) Normalized TOC decay vs. electrolysis time for the assays of Fig. 2 (initial TOC of 50 mg L^{-1}). Concentration of (b) accumulated ammonium ion and (c) chloride ion during the same trials. Method: (○) EO-H_2O_2, (□) EF and (▲) PEF.

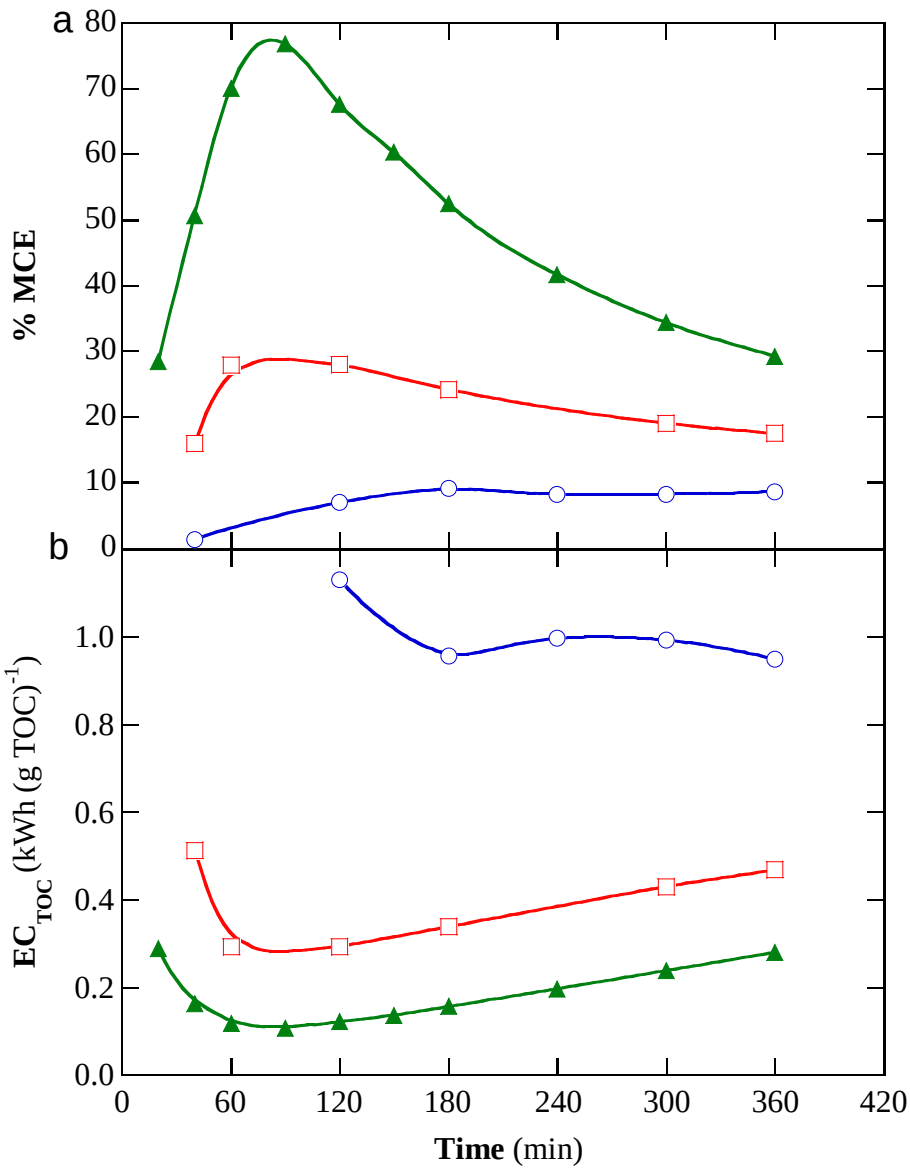

Fig. 4. Change of (a) percentage of mineralization current efficiency and (b) energy consumption per unit TOC mass with electrolysis time for the experiments of Fig. 3a. Method: (○) EO-H_2O_2), (□) EF and (▲) PEF.

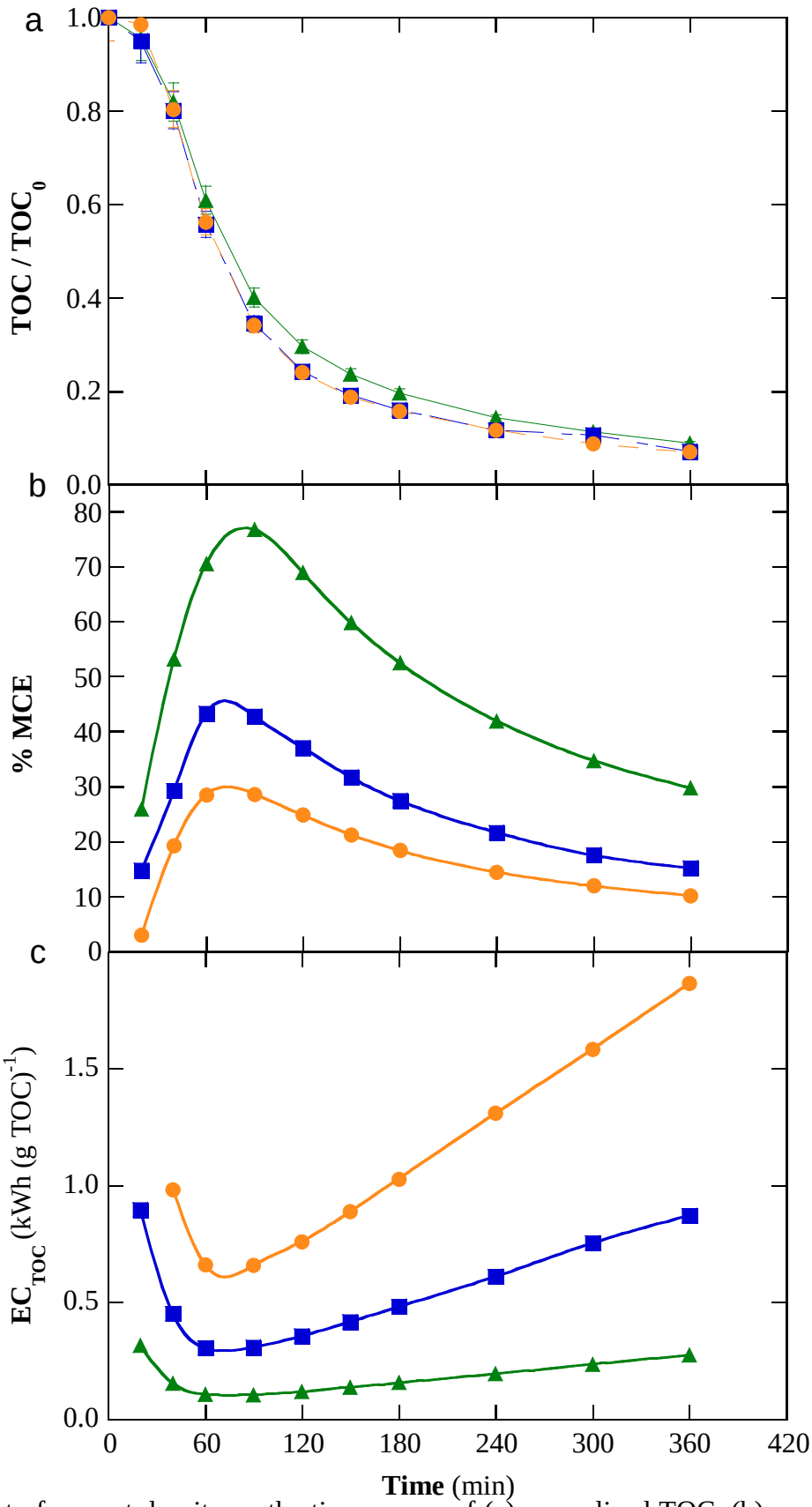

Fig. 5. Effect of current density on the time course of (a) normalized TOC, (b) percentage of mineralization current efficiency and (c) energy consumption per unit TOC mass for the PEF treatment of 2.5 L of a 0.320 mM procaine hydrochloride solution with 0.050 M Na_2SO_4 and 0.50 mM Fe^{2+} at pH 3.0 and 35 ºC using a pre-pilot flow plant with a BDD/air-diffusion cell at liquid flow rate of 180 L h^{-1}. Applied *j*: (▲) 33.3 mA cm^{-2}, (■) 66.7 mA cm^{-2} and (●) 100 mA cm^{-2}.

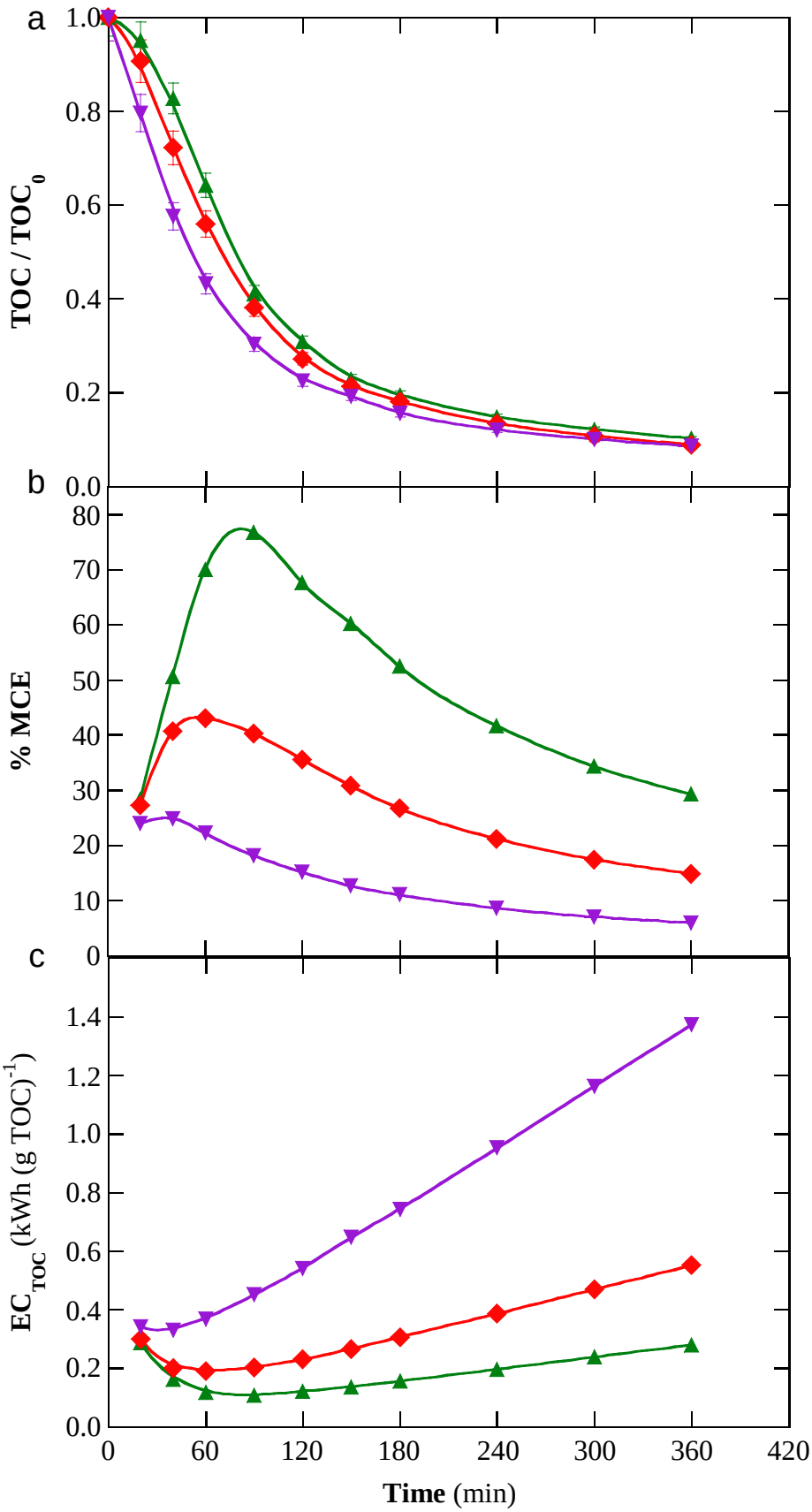

Fig. 6. Influence of drug concentration on the time course of (a) normalized TOC, (b) percentage of mineralization current efficiency and (c) energy consumption per unit TOC mass for the PEF treatment of 2.5 L of procaine hydrochloride solutions with 0.050 M Na_2SO_4 and 0.50 mM Fe^{2+} at pH 3.0 and 35 ºC using a pre-pilot flow plant with a BDD/air-diffusion cell at j = 33.3 mA cm^{-2} and liquid flow rate of 180 L h^{-1}. Drug content: (▼) 0.064 mM, (◆) 0.160 mM and (▲) 0.320 mM.

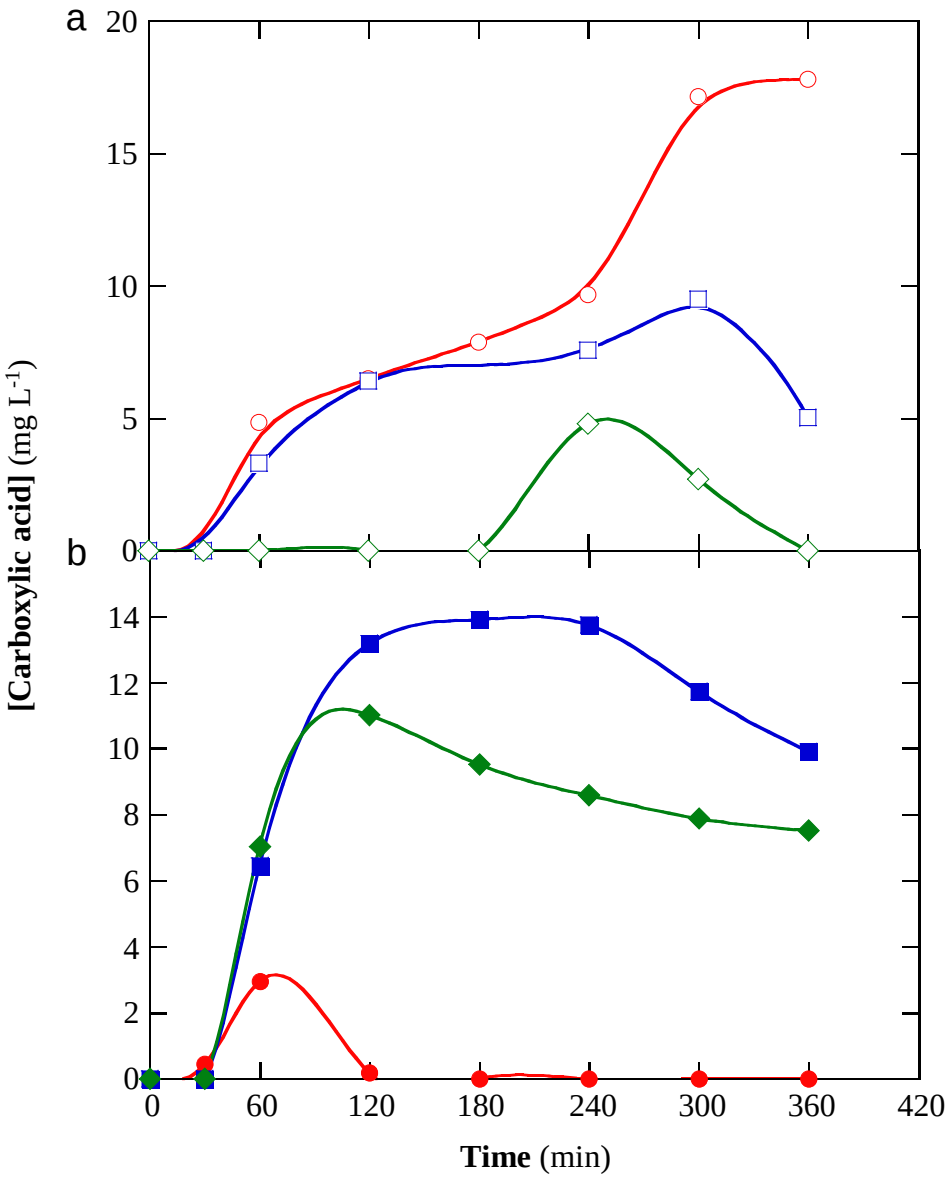

Fig. 7. Change of the concentration of (○,●) oxalic, (□,■) formic and (◇,◆) acetic acids detected during the (a) EF and (b) PEF treatments of 2.5 L of 0.320 mM procaine hydrochloride solutions with 0.050 M Na_2SO_4 and 0.50 mM Fe^{2+} at pH 3.0 and 35 ºC using a pre-pilot flow plant with a BDD/air-diffusion cell at j = 33.3 mA cm^{-2} and liquid flow rate of 180 L h^{-1}.

Table 1. Characteristics of the aromatic compounds detected by GC-MS with a non-polar column during the EO-H_2O_2 treatment of 2.5 L of a 0.320 mM procaine hydrochloride solution in 0.050 M Na_2SO_4 at pH 3.0 and 35 ºC using a pre-pilot flow plant with a BDD/air diffusion cell at j = 33.3 mA cm^{-2} and liquid flow rate of 180 L h^{-1}.

Number	Chemical name	Molecular structure	Retention time (min)	Main fragmentation ions (*m*/*z*)
1	2-(Diethylamino)ethyl-4-aminobenzoate (Procaine)	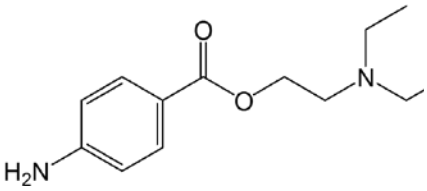	36.92	235, 164, 137, 120, 99, 86
2	2-(Diethylamino)ethyl-4-nitrobenzoate	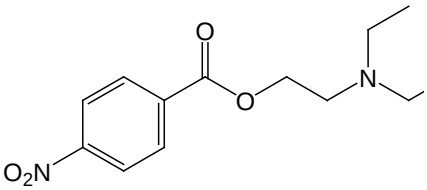	35.88	266, 194, 150, 120, 86, 76
3	Ethyl-4-nitrobenzoate	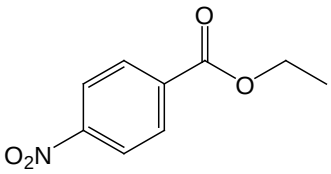	38.95	195, 150, 120, 104, 92, 76